

PAPER • OPEN ACCESS

Electronic properties and degradation upon VUV irradiation of sodium chloride on Ag(111) studied by photoelectron spectroscopy

To cite this article: Haibo Wang *et al* 2021 *Electron. Struct.* **3** 034008

View the [article online](#) for updates and enhancements.

You may also like

- [Dependence of the NaCl/Au\(111\) interface state on the thickness of the NaCl layer](#)
Koen Lauwaet, Koen Schouteden, Ewald Janssens *et al.*
- [Mg-RE Alloy Anode Materials for Mg-Air Battery Application](#)
N. Shrestha, K. S. Raja and V. Utgikar
- [Experimentally determined and Monte Carlo-calculated energy dependence of NaCl pellets read by optically stimulated luminescence for photon beams in the energy range 30 keV to 1.25 MeV](#)
Lovisa Waldner, Christopher Rääf, Yvonne Hinrichsen *et al.*

Electronic Structure

OPEN ACCESS**PAPER**

Electronic properties and degradation upon VUV irradiation of sodium chloride on Ag(111) studied by photoelectron spectroscopy

RECEIVED
30 June 2021REVISED
26 July 2021ACCEPTED FOR PUBLICATION
7 September 2021PUBLISHED
22 September 2021

Original content from this work may be used under the terms of the [Creative Commons Attribution 4.0 licence](#).

Any further distribution of this work must maintain attribution to the author(s) and the title of the work, journal citation and DOI.



Haibo Wang^{1,2} , Martin Oehzelt^{1,3} , Stefanie Winkler^{1,3} , Ruslan Ovsyannikov⁴ , Norbert Koch^{1,3} and Patrick Amsalem^{1,*}

¹ Institut für Physik and IRIS Adlershof, Humboldt-Universität zu Berlin, Berlin, Germany

² School of Materials Science and Engineering, Jilin University, Changchun 130012, People's Republic of China

³ Helmholtz-Zentrum Berlin für Materialien und Energie GmbH, BESSY II, Berlin, Germany

⁴ Institute for Methods and Instrumentation in Synchrotron Radiation Research PS-ISRR, Helmholtz-Zentrum Berlin für Materialien und Energie GmbH, Berlin, Berlin 12489, Germany

* Author to whom any correspondence should be addressed.

E-mail: amsalem@physik.hu-berlin.de

Keywords: photoemission, sodium chloride (NaCl), irradiation damage, photon stimulated desorption, work function

Abstract

The growth as well as vacuum ultraviolet (VUV) radiation-induced degradation of sodium chloride (NaCl) on Ag(111) is investigated by ultraviolet and x-ray photoelectron spectroscopy. In line with previous scanning tunneling microscopy studies, our results confirm that NaCl grows initially as a bilayer before island growth starts. Simple spectroscopic methods for calibrating the closure of the NaCl bilayer are further presented. In addition, the energy level alignment is studied as a function of NaCl film thickness and VUV-light intensity. When measuring with ultra-low photon flux, a sharp interface dipole lowers the sample work function by 0.65 eV upon adsorption of the first bilayer, which is followed by vacuum level alignment for subsequently deposited layers. In contrast, measurements performed with standard photon fluxes, such as those provided by commercial He discharge lamps, shows ‘downward band-bending’-like characteristics in the NaCl films. Upon extended exposure time to the standard VUV intensity, photoemission measurements further reveal that strong modifications of the electronic properties of the NaCl surface occur. These are likely correlated with halogen emission, eventually resulting in the formation of Na clusters promoting low work function of parts of the sample surface. This study provides general guidelines for obtaining reliable spectroscopic measurements on alkali halide thin films on metals.

Introduction

Nowadays development of opto-electronic devices goes with increasing heterostructure complexity, comprising many heterojunctions commonly including electrode/semiconductor and semiconductor/semiconductor interfaces. In addition, the insertion of buffer layers in between the electrode and the semiconductor has become ubiquitous to overcome poor charge injection/extraction [1–3], a major issue of organic-based devices [4–6]. Counterintuitively, the use of *insulating* layers consisting of alkali halides inserted in between the metal cathode and the *n*-type organic semiconductor has proven successful to minimize energy losses at these interfaces and is now widely employed, notably in organic photovoltaic solar cells [7] and organic light emitting diodes [8] but also in organic field-effect transistors [9] and transistor memory [10]. As pointed out by different studies, the predominant underlying mechanism responsible for device improvement has been strongly debated and may be notably correlated to (i) the tuning of the electrode work function [8]; (ii) the presence of band-bending within the salt layer [11, 12]; (iii) the emergence of a spatially extended band bending in the active (organic) materials [13]; (iv) the doping of the organic materials by alkali atoms upon thermal evaporation of alkali halides thin films [14].

Ultra-violet and x-ray photoelectron spectroscopy (UPS and XPS) are techniques of choice to investigate the electronic and chemical properties of thin films and, therefore to understand the role of buffer layers in devices and the structure-property relationship of films grown on metal electrodes [13, 15, 16]. However, the use of UPS and XPS is challenging for such studies as large band-gap ionic insulators can retain strong sample charging and further degradation may occur upon UV-light or electron irradiation [17–20]. In addition, though it is well-known that the interaction of photon or electron beams with alkali halides leads to atomic desorption and consequent surface restructuring, the effects induced by vacuum ultraviolet (VUV) light, i.e., in the energy range typically used photoemission measurements, on the electronic and chemical properties of interfaces including alkali halides thin films have been barely addressed so far [21].

Among alkali halides, sodium chloride (NaCl) is a prototypical wide band gap insulator, which can exhibit the bulk crystal gap already at bi-layer thickness [22]. NaCl is also known from scanning tunneling microscopy measurements to form continuous and smooth carpet-like films with (100) orientation covering the monatomic steps of substrates such as Ag(111) [23]. This makes the use of NaCl thin films common for probing the fundamental optoelectronic properties of atomic or molecular adsorbates decoupled from a supporting metal electrode [13, 24–27].

In this work, we study by photoelectron spectroscopy (PES) the thickness-dependent electronic properties of a NaCl film grown on Ag(111). First, we look at the growth mode and confirm that a bilayer growth occurs before island formation starts, in agreement with previous microscopy studies and further propose a simple method to determine the completion of the first NaCl bilayer. In a second step, the electronic structure as probed by PES is investigated as a function of film thickness and VUV-light fluence. We show that, in addition to the formation of an interface dipole, the energy level alignment goes from vacuum level alignment to apparent strong band-bending, whose magnitude depends on the photon flux used during the measurement. Finally, the effect of high dose of VUV-light irradiation as provided by the HeI radiation of standard helium discharge lamps on a 10 nm NaCl thick film is addressed. It is shown to induce a large number of defects, eventually leading to local surface restructuring going with the formation of Na clusters as deduced from the valence band and work function changes upon VUV-light exposure.

1. Experimental

The samples were prepared and analyzed *in situ* under ultra-high vacuum conditions. The Ag(111) surface was cleaned by several Ar⁺ sputtering and annealing (750 K) cycles. NaCl (Aldrich, 99.99% pure) was evaporated from resistively heated crucibles at 500 °C. The film thickness was monitored with a quartz microbalance using a density for NaCl of 2.165 g cm⁻³. The HeI radiation (21.22 eV) from a He discharge lamp [Specs, UVS 10/35 providing ca 8 × 10¹⁵ photons/(s*sr) and yielding a sample current density J_s of ca 100 pA mm⁻² for a clean Ag(111) sample] was used for in-house ultraviolet photoelectron spectroscopy (UPS) in combination with an Omicron EA125 hemispherical energy analyzer (120 meV energy resolution). For in-house measurements, an attenuation of the UV-light intensity by one order of magnitude was obtained by inserting a 300 nm thin aluminum filter between the lamp capillary and the sample. High resolution XPS ($h\nu = 1500$ eV) and ‘ultra-low photon flux’ UPS ($h\nu = 21$ eV, with intensity reduced by two order of magnitude as compared to that provided by the helium lamp) measurements were performed using synchrotron radiation at the former SurICat end station (beamline PM4) equipped with a Scienta SES 100 hemispherical analyzer at the BESSY II synchrotron light source (Berlin, Germany). The flux reduction were determined from the sample current density measured upon illumination of the clean Ag(111) ($J_s \sim 10$ pA mm⁻² with aluminum filter and ~ 1 pA mm⁻² for the ‘ultra-low flux’). If not explicitly stated, all the UPS and XPS spectra were collected in normal emission, and the electron binding energies are referred to the silver Fermi level. Secondary electron cut-off (SECO, for determination of sample work function) spectra were collected with a -10 V bias applied to the sample.

2. Results and discussion

2.1. Growth of NaCl on Ag(111)

We first investigate the growth of NaCl on Ag(111) with an emphasis on the NaCl/Ag(111) very interface region. We also provide hints for the calibration of NaCl film closure by means of UPS.

Figure 1(a) displays the thickness-dependent Na KLL Auger spectra of NaCl adsorbed on Ag(111). The thick film spectrum (10 nm NaCl) is representative of the bulk characteristics of NaCl. The corresponding Na KLL Auger peak is composed of two features consisting of a main peak at ca 985.75 eV kinetic energy (KE) and a smaller one at 981 eV KE. When investigating the interface properties, the shape of the Na KLL

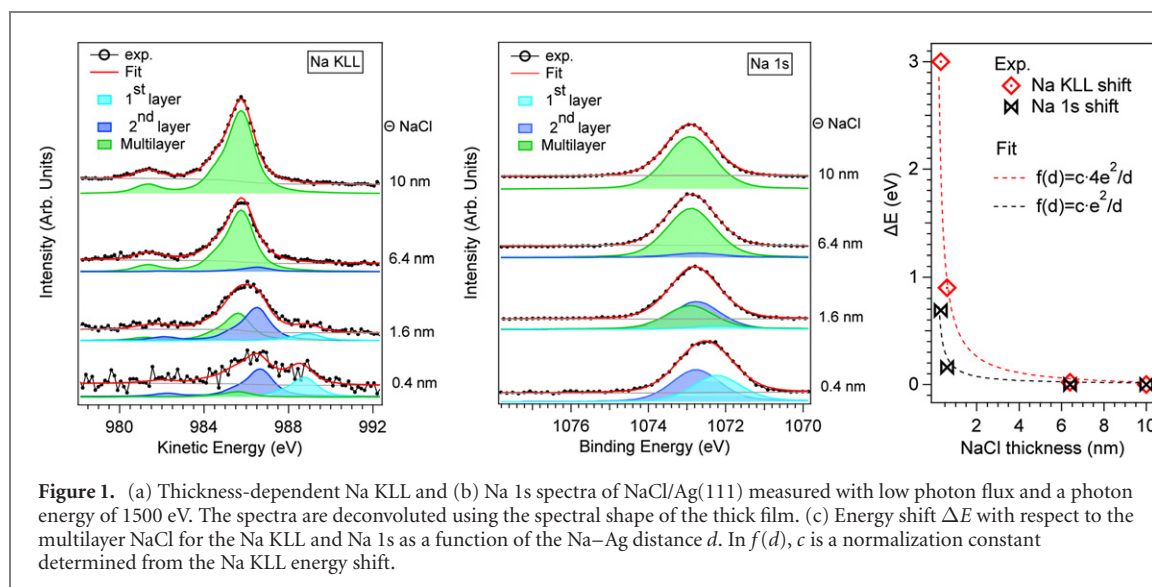


Figure 1. (a) Thickness-dependent Na KLL and (b) Na 1s spectra of NaCl/Ag(111) measured with low photon flux and a photon energy of 1500 eV. The spectra are deconvoluted using the spectral shape of the thick film. (c) Energy shift ΔE with respect to the multilayer NaCl for the Na KLL and Na 1s as a function of the Na–Ag distance d . In $f(d)$, c is a normalization constant determined from the Na KLL energy shift.

spectrum appears markedly different, with the notable presence of an intense shoulder at ca 989 eV KE. The fitting procedure using several Na KLL contributions derived from the bulk spectrum and shown in figures 1(a) and (b) for 0.4 nm (nominally 0.66 bilayer) and 1.6 nm (nominally 2.66 bilayers or 5.33 monolayer) NaCl helps disentangle the different interface and bulk features. A good fit is only achieved by considering that these experimental spectra are actually composed of three well-separated contributions with their main peak at 988.75 eV KE, 986.65 eV KE and 985.75 eV KE as it is markedly apparent for 1.6 nm NaCl (figure 1(a)). These different contributions are therefore readily identified as stemming from the very first NaCl layer (988.75 eV KE) in contact with the metal substrate, the second NaCl layer (986.5 eV KE) and the multilayer (985.75 eV KE). Considering that the mean free path for electrons around 985 eV KE is ca 1.5–2 nm, for 0.4 nm NaCl, the intensity ratio between the different components as determined with the fitting procedure indicates that NaCl grows mostly in a bilayer fashion (owing to the formation of a small density of 3D island as suggested by the low KE peak) until the closure of the first NaCl bilayer is reached, consistently with previous reports on the growth at room temperature of NaCl on Ag(111) and other close-packed surfaces of noble metals [23, 28].

In contrast, these different contributions are hardly distinguishable in the Na 1s core level spectra as shown in figure 1(b). There, we fitted the core level assuming that, as for the Na KLL, the Na 1s peak lineshape is not noticeably modified by the proximity of the surface. Based on this assumption, we find that the multilayer, second layer and first layer NaCl peaks are located at 1072.92 eV, 1072.77 eV and 1072.23 eV binding energy (BE), respectively. As no chemical shift due to interfacial charge transfer is *a priori* expected [as for instance indicated by the virtually identical Ag3d lineshape for clean and NaCl-covered Ag(111) (not shown)], the energy shift ΔE between the different layers is likely to originate only from differential photohole screening by the metal electrons, promoting thereby higher kinetic energy to the electrons emitted from the atoms in close contact with the metal surface. To verify this hypothesis, we examined in figure 1(c) the energy shift ΔE of the probed Auger and core level (photo-) electrons as a function of d , the distance of the probed atom to the metal surface. In this context, ΔE is expected to vary as q^2/d , where q represents the charge of the atom in the final state with respect to the ground state. Therefore, ΔE for the Auger electrons, because of the doubly-ionized final state of the probed atoms, should be four times larger than that of the singly ionized core level photoelectrons. The results shown in figure 1(c), show that ΔE for both Na KLL and Na 1s verify (within error) that ΔE varies like $1/d$ and that $\Delta E_{\text{Na KLL}} = 4 \cdot \Delta E_{\text{Na 1s}}$ which demonstrates that the observed energy shifts indeed mostly result from differential photohole screening by the metal electrons and do not stem for instance from charge transfer or chemical interaction between NaCl and the silver surface.

To further assess the growth behavior, we also monitored the relative evolution of the Na 1s and Ag 3d intensities as a function of film thickness as displayed in figure 2(a). In this graph, the change in slope at 0.6 nm NaCl thickness for both the Ag and Na signal indicates the completion of the first bilayer in excellent agreement with the NaCl lattice constant of 0.56 nm and with the analysis of the Na KLL/Na 1s spectra. Thereafter, the evolution of the relative intensities suggests that island growth starts, resulting in a Stranski–Krastanov growth mode.

We also looked at the valence features, searching for some hints of the closure of the first NaCl bilayer. Figure 2(b) shows the Ag(111) Fermi edge measured in UPS in normal emission and at 10° off-normal emission. The normal emission spectrum of clean Ag(111) exhibits an intense feature stemming from the Shockley

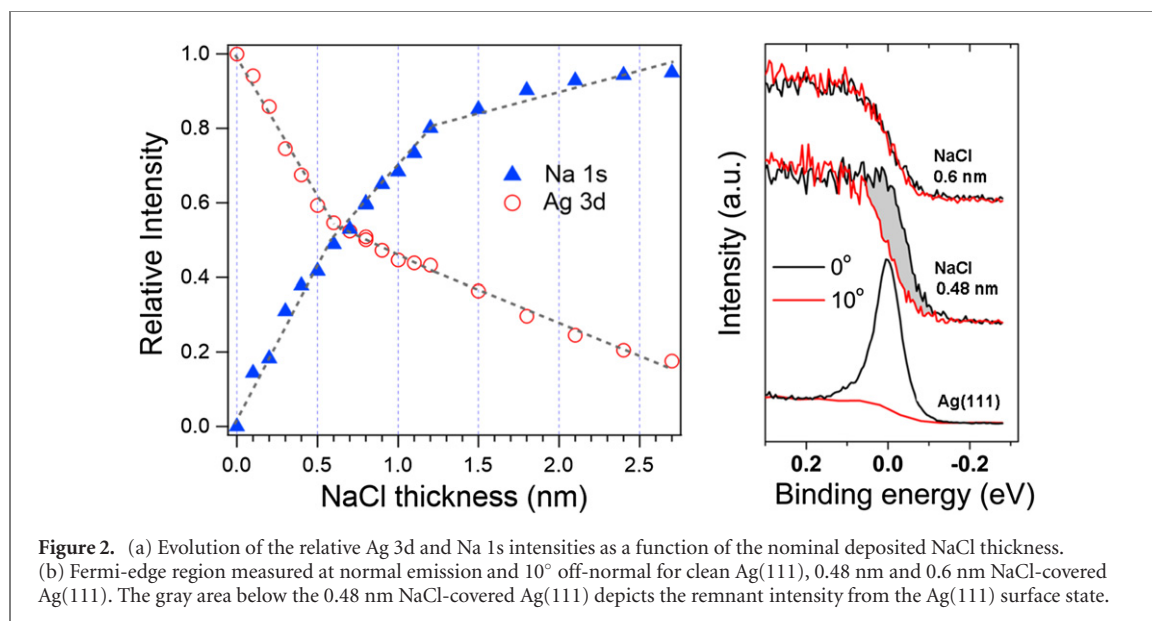


Figure 2. (a) Evolution of the relative Ag 3d and Na 1s intensities as a function of the nominal deposited NaCl thickness. (b) Fermi-edge region measured at normal emission and 10° off-normal for clean Ag(111), 0.48 nm and 0.6 nm NaCl-covered Ag(111). The gray area below the 0.48 nm NaCl-covered Ag(111) depicts the remnant intensity from the Ag(111) surface state.

surface state, followed by a flat density of states (DOS) at higher BE due to the Ag *sp*-band. Slightly off-normal emission (10°), the surface state vanishes completely as it is strongly centered around the Gamma point of the Brillouin zone [29]. When incrementally depositing NaCl, a progressive quenching of the surface state is observed. This is in line with corresponding scanning tunneling spectroscopy measurements of the NaCl/Ag(111) interface and with other reports on the adsorption of weakly interacting organic molecules on Ag(111), for which the Shockley surface state is known to shift above the Fermi-level [30–32]. At 0.48 nm NaCl, i.e. when approaching the completion of the bilayer film (ca 80% of a full bilayer) as determined by XPS, the normal emission spectrum displays only a flat band which could be attributed to the complete quenching of the surface state. However, a careful comparison with the 10° take-off angle spectrum reveals an apparent shift of the Fermi-edge in the normal emission spectrum. This discrepancy is due to remnant DOS from the surface states which is superimposed on the bulk-like silver DOS. Finally, for 0.6 nm NaCl/Ag(111), the surface state is completely vanished as shown by the virtually identical lineshape and energy position of the Fermi-edge spectra for both emission angles. Remarkably, this happens at the same NaCl thickness as the one determined by XPS for a complete NaCl bilayer. Therefore, we conclude that the attenuation of the surface state as measured in UPS can be used as a simple and precise tool for calibrating the closure of the first NaCl bilayer.

2.2. Effect of light fluence on the energy level alignment

We now examine the energy level alignment at the NaCl/Ag(111) interface as observed by UPS. First, we recorded the thickness-dependent valence band spectra under standard photon flux (referred to as ‘without filter’ in figure 3(a)) as provided by a commercial helium discharge lamp with specifications detailed in the Experimental section. The selected spectra which are shown in figure 3(a) exhibit two peaks (labeled A and B) which are due to the Cl 3p levels. With increasing thickness, the whole valence band progressively shifts to higher BE by up to 2.1 eV, which could in principle be ascribed to charging of the molecular film or, alternatively, to band-bending phenomena as previously suggested. The graph in figure 3(d) reports the thickness-dependent energy shift of peak A together with the sample work function evolution, which decreases from 4.5 eV for clean Ag(111) down to 2.4 eV for the range of investigated thicknesses. This comparison highlights the fact that both the valence band features and the work function mostly shift in a rigid manner.

Figures 3(b) and (c) show the valence band evolution when performing UPS measurements with photon flux defined as ‘with filter’ and ultra-flux’, which are reduced by 1 and 2 orders of magnitude as compared to the ‘without filter’ photon flux, respectively. The graph in figure 3(d) also reports the work function evolution and the energy shift of peak A for these measurements. When using a photon flux reduced with filter, the valence band and work function shift by 1 eV for a film thickness of 20 nm, which is only half as much as what was detected with standard photon flux. For the ultra-low photon flux case ($J_s \sim 1 \text{ pA mm}^{-2}$), a total work function shift of 0.65 eV is observed upon interface formation, which is followed by vacuum level alignment for the subsequently deposited layers. This interface dipole is mostly due to the push-back effect, i.e., the push-back of the electrons spilling out the metal surface [33, 34], and its magnitude is in-line with the usual observations at weakly interacting adsorbate on Ag(111) [32]. In addition, the reliability of the ultra-low photon flux measurements is confirmed by noting that work function behavior as determined by Kelvin probe force microscopy, a non-destructive technique, for different thicknesses of NaCl island on Ag(100) is quantitatively the same [35].

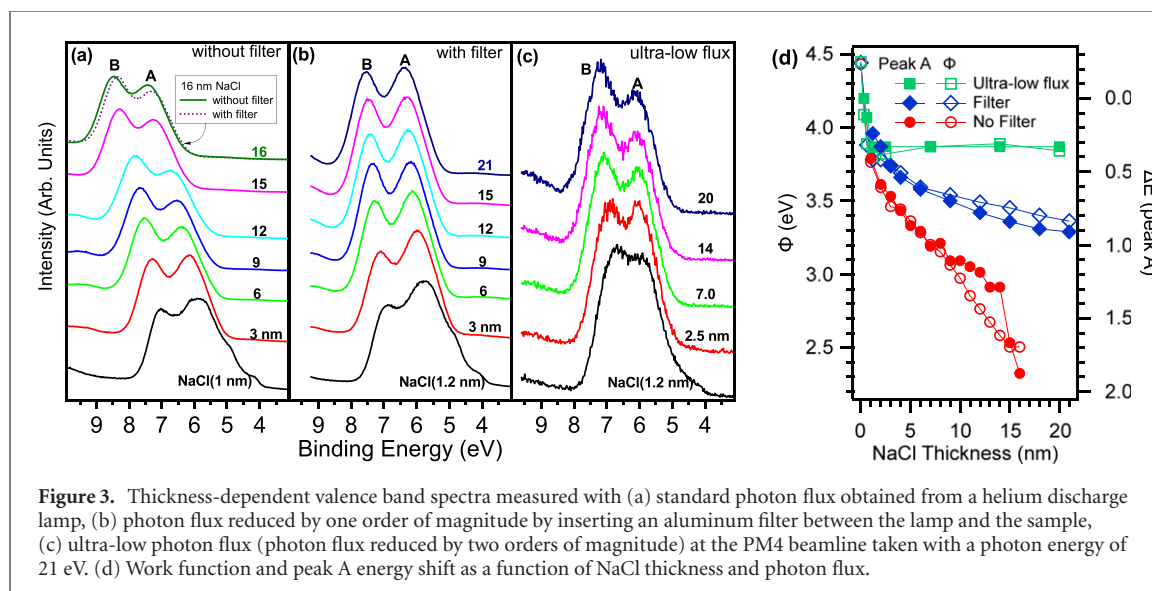


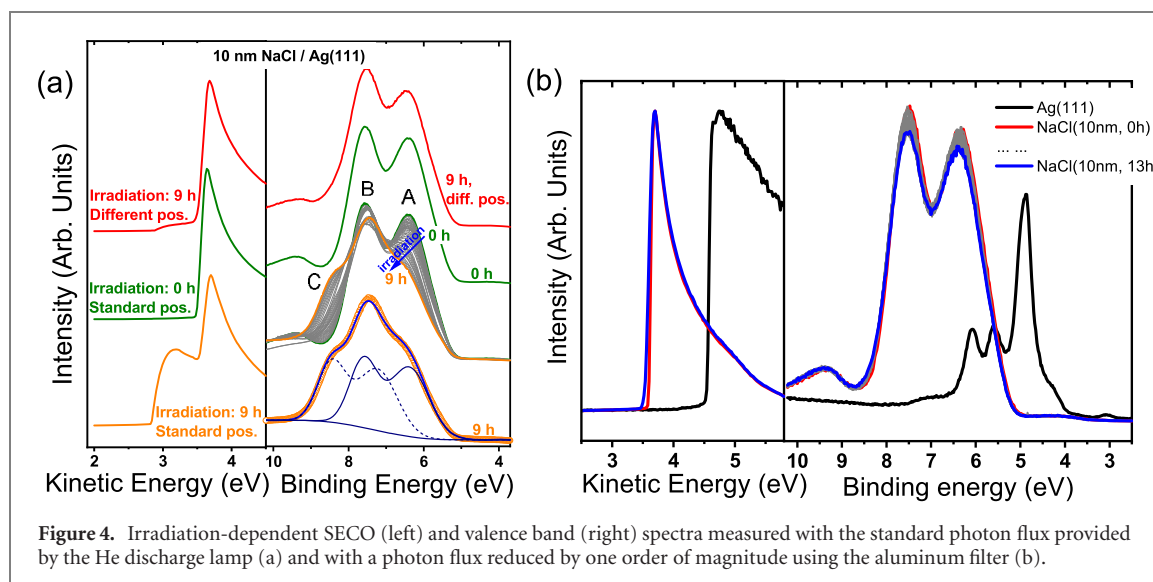
Figure 3. Thickness-dependent valence band spectra measured with (a) standard photon flux obtained from a helium discharge lamp, (b) photon flux reduced by one order of magnitude by inserting an aluminum filter between the lamp and the sample, (c) ultra-low photon flux (photon flux reduced by two orders of magnitude) at the PM4 beamline taken with a photon energy of 21 eV. (d) Work function and peak A energy shift as a function of NaCl thickness and photon flux.

Therefore, we demonstrated that the band alignment determined in UPS varies dramatically as a function of the VUV-light fluence and that the apparent band-bending is related to charging/degradation of the film. The comparison between two spectra acquired first with high and then with low photon flux on the same sample as displayed in figure 3(a) further show that the shift induced with standard measurement conditions is not reversible upon reduction of the photon flux which suggests that, beyond simple charging, degradation of the film via formation of charged defects occurs. Therefore, charged defect formed and accumulated at the film surface at each deposition step, which then resulted in large, dose-dependent, change of the electrostatic potential within the film as seen in figure 3(d). In contrast, when ‘ultra-low’ photon dose such as that employed here, no such defects formed as demonstrated by the constant potential measured at each deposition step.

2.3. NaCl degradation upon VUV-light irradiation

To explore more in detail the effect of UV-light-induced damage, we recorded the evolution of the valence band of a 10 nm NaCl film on Ag (111) over exposure time as displayed in figure 4(a). The initial NaCl valence band features are entirely due the Cl $3p_{3/2}$ (peak B) and Cl $3p_{1/2}$ (peak A). Upon irradiation for an extended amount of time, the valence band strongly evolves and features the emergence of an additional component, denoted peak C at 8.5 eV BE, as well as the progressive quenching of peak A. At the same time, the intensity of peak B remains approximately constant. An explanation for the evolution of the valence band spectra over time is further provided in figure 4(a) with a fitting of the valence band after exposure using the initial spectrum duplicated, appropriately shifted in energy and scaled in intensity. This analysis reveals that all the changes in the valence features described above are actually due to a duplication of the valence band features toward higher BE: the initial features decrease in intensity when, at the same time, the equivalent Cl $3p$ contributions shifted by 0.9 eV to higher BE increasingly grows. After 9 h of VUV exposure, the fraction of shifted and pristine valence band features amounts to ca 50% each.

After nine hours, the SECO spectrum also shows major change with the emergence of a double SECO, indicating two distinct surface work functions Φ_1 and Φ_2 . Φ_1 is mostly unchanged as compared to the initial value of 3.48 eV at $t = 0$ h and the second SECO is representative of $\Phi_2 = 2.82$ eV, i.e. 0.66 eV smaller than Φ_1 . The emergence of a double SECO is a clear indication of local work function inhomogeneity at the sample surface with the presence of two distinct areas: Φ_1 corresponds to the pristine parts of the sample surface while Φ_2 relates an area-averaged value of the fractions of modified and unchanged surface such that $\Phi_2 = \alpha\Phi_1 + \beta\Phi_2^*$, where α and β are the fractions of intact and degraded surface areas and Φ_2^* is the local work function of the degraded areas [36, 37]. On one hand, it is tempting to correlate α and β with the share of pristine and shifted valence feature as deduced from the valence band analysis ($\alpha \approx \beta \approx 0.5$), which would result in Φ_2^* of 2.15 eV, i.e., a value slightly smaller than the lowest reported value of Na of 2.27 eV, and providing a lower estimate of the true Φ_2^* [38, 39]. On the other hand, one may correlate the energy shift of part of the valence band features directly with the change in surface potential, yielding Φ_2^* of 2.6 eV, close to the 2.7 eV work function of free Na nanoparticles reported by Wong *et al* [38, 40]. From this, we can calculate that the fraction of degraded areas β correspond to ca 25% of the exposed surface, which would be consistent with the lower SECO intensity of the low work function areas as compared to that of the pristine areas. In any case, these observations points toward the fact that the low work function areas induced by VUV exposure should



be correlated with an accumulation of Na atoms at the surface forming metallic clusters, consistently with a number of previous works concluding on the formation of alkali clusters at the surface of photon or electron irradiated NaCl and other alkali halides [17, 18, 21, 41–43]. However, we note that we did not observe any obvious sign of DOS related to metallic Na at the Fermi level, which may eventually indicate that we overestimated the magnitude of β , the fraction of degraded areas. If so, this overestimate could likely be a result of the lateral extend of the potential drop around the Na clusters, which was not accounted for in the above reasoning. The two main mechanisms leading to formation of Na metal clusters can be summarized as follow: (i) electrons and holes, created in the bulk upon irradiation, can be self-trapped resulting in a pair of F (an electron trapped in halogen vacancy) and H (an interstitial halogen atom) centers; those pairs then diffuse to the surface where thermal emission of the halogen and neutralization of the surface alkali occur [19, 42]. (ii) Hot hole–electron pairs are formed upon photon absorption; those pairs diffuse to the NaCl surface and, if the hole is located on the surface halogen atom, the canceling of the Coulombic bond leads to the ejection of the chlorine atom due to Pauli repulsion by the electron cloud, a mechanism also known to induce preferential non-thermal desorption of halogen atoms and neutral alkali atoms [17, 41, 42, 44]. Such phenomena were shown to induce surface restructuring including layer-by-layer desorption of NaCl and the formation of 2D rectangular pits at the film surface [42, 45]. As suggested by previous atomic force microscopy studies, the Na adatoms then diffuse and start agglomerating at the pit edges and kinks [42]. Extrapolating, our data may therefore suggest that irradiation induces the formation of a large amount of pits, which gives rise to a significant fraction of the surface being covered by Na clusters. Finally, we also performed the same experiment using the attenuated photon flux using the aluminum filter as in figure 4(b). The results presented in this figure show that, upon illumination with the reduced photon flux, no evolution of the spectrum occurs over time, which enables the possibility to perform long photoemission measurements without further sample changes.

3. Conclusion

In this study, we investigated by photoemission the growth of NaCl on Ag(111) and found that, consistently with previous reports, that NaCl thin films initially grow as a bilayer on the Ag(111) surface. The large energy shift observed of the core levels and Auger electrons for the first, second and subsequent NaCl layers can be consistently attributed to final state screening by the metal electrons, ruling out changes in the oxidation state of NaCl by charge transfer. The observation of quenching of the Ag(111) surface state is also shown to be a simple and precise way of estimating the closure of the first NaCl bilayer. The energy line-up for thicknesses ranging from ultrathin up to 20 nm thick NaCl films was then studied employing different photon fluxes. A reliable assessment of the energy level alignment could only be achieved by decreasing the photon flux of a standard He lamp by two order of magnitudes. In this experimental condition, we observed the formation of an interface dipole due to the push-back effect followed by vacuum level alignment. In contrast, using higher photon fluences induces irreversible charging/damage to the alkali halide films and leads to an apparent downward band-bending. Time-dependent studies further reveal that high irradiation doses strongly alter the surface electronic properties, leading to a strongly laterally inhomogenous sample work function. This is proposed to

go in hand with the formation of Na clusters and halide desorption. This effect could potentially be used for work function patterning of alkali halide thin films in the future.

Acknowledgments

The Deutsche Forschungsgemeinschaft (DFG), Projektnummer 182087777, SFB 951 is gratefully acknowledged for financial support.

Data availability statement

The data that support the findings of this study are available upon reasonable request from the authors.

ORCID iDs

Haibo Wang  <https://orcid.org/0000-0002-0485-6477>
Martin Oehzelt  <https://orcid.org/0000-0002-9646-6889>
Ruslan Ovsyannikov  <https://orcid.org/0000-0001-6311-5516>
Norbert Koch  <https://orcid.org/0000-0002-6042-6447>
Patrick Amsalem  <https://orcid.org/0000-0002-7330-2451>

References

- [1] Allen T G, Bullock J, Yang X, Javey A and De Wolf S 2019 Passivating contacts for crystalline silicon solar cells *Nat. Energy* **4** 914–28
- [2] Wan S, Zhang G, Niederhausen J, Wu D, Wang Q, Sun B, Song T and Duhm S 2021 Schottky contact formation by an insulator: lithium fluoride on silicon *Appl. Phys. Lett.* **118** 241601
- [3] Schultz T, Lungwitz D, Longhi E, Barlow S, Marder S R and Koch N 2021 The interlayer method: a universal tool for energy level alignment tuning at inorganic/organic semiconductor heterojunctions *Adv. Funct. Mater.* **31** 2010174
- [4] Grem G, Leditzky G, Ullrich B and Leising G 1992 Realization of a blue-light-emitting device using poly (p-phenylene) *Adv. Mater.* **4** 36–7
- [5] Hung L S, Tang C W and Mason M G 1997 Enhanced electron injection in organic electroluminescence devices using an Al/LiF electrode *Appl. Phys. Lett.* **70** 152–4
- [6] Kotadiya N B, Lu H, Mondal A, Ie Y, Andrienko D, Blom P W M and Wetzelaer G-J A H 2018 Universal strategy for ohmic hole injection into organic semiconductors with high ionization energies *Nat. Mater.* **17** 329–34
- [7] Brabec C J, Shaheen S E, Winder C, Sariciftci N S and Denk P 2002 Effect of LiF/metal electrodes on the performance of plastic solar cells *Appl. Phys. Lett.* **80** 1288–90
- [8] Brown T M, Friend R H, Millard I S, Lacey D J, Butler T, Burroughes J H and Cacialli F 2003 Electronic line-up in light-emitting diodes with alkali-halide/metal cathodes *J. Appl. Phys.* **93** 6159–72
- [9] Ma L and Yang Y 2004 Unique architecture and concept for high-performance organic transistors *Appl. Phys. Lett.* **85** 5084–6
- [10] Wang S, Chan P K L, Leung C W and Zhao X 2012 Controlled performance of an organic transistor memory device with an ultrathin LiF blocking layer *RSC Adv.* **2** 9100–5
- [11] Schlaf R, Parkinson B A, Lee P A, Nebesny K W, Jabbour G, Kippelen B, Peyghambarian N and Armstrong N R 1998 Photoemission spectroscopy of LiF coated Al and Pt electrodes *J. Appl. Phys.* **84** 6729–36
- [12] Sun Z, Shi S, Bao Q, Liu X and Fahlman M 2015 Role of thick-lithium fluoride layer in energy level alignment at organic/metal interface: unifying effect on high metallic work functions *Adv. Mater. Interfaces* **2** 1400527
- [13] Wang H, Amsalem P, Heimel G, Salzmann I, Koch N and Oehzelt M 2014 Band-bending in organic semiconductors: the role of alkali-halide interlayers *Adv. Mater.* **26** 925–30
- [14] Hung L S, Zhang R Q, He P and Mason G 2001 Contact formation of LiF/Al cathodes in Al q-based organic light-emitting diodes *J. Phys. D: Appl. Phys.* **35** 103–7
- [15] Yang J, Wang Q, Wan S, Wu D, Chen M, Kashtanov S and Duhm S 2021 Photoelectron spectroscopy reveals molecular diffusion through physisorbed template layers on Au(111) *Electron. Struct.* **3** 024002
- [16] Hurdax P, Hollerer M, Puschnig P, Lüftner D, Egger L, Ramsey M G and Sterrer M 2020 Controlling the charge transfer across thin dielectric interlayers *Adv. Mater. Interfaces* **7** 2000592
- [17] Friedenberga A and Shapira Y 1979 Electron induced dissociation of the NaCl(111) surface *Surf. Sci.* **87** 581–94
- [18] Durrer W G, Portillo M, Wang P and Russell D P 1994 Temperature dependence of surface charging of NaCl under electron irradiation: role of secondary electron emission *Appl. Surf. Sci.* **81** 215–21
- [19] Kolodziej J J et al 2001 Frenkel defect interactions at surfaces of irradiated alkali halides studied by non-contact atomic-force microscopy *Surf. Sci.* **482–485** 903–9
- [20] Szymonski M, Droba A, Goryl M, Kolodziej J J and Krok F 2006 Alkali halide decomposition and desorption by photons—the role of excited point defects and surface topographies *J. Phys.: Condens. Matter* **18** 1547S–62
- [21] Owaki S, Koyama S, Takahashi M, Kamada M and Suzuki R 1997 Metallic Na formation in/on NaCl crystals with irradiation by electron or vacuum ultraviolet photons *Radiat. Phys. Chem.* **49** 609–15
- [22] Kramer J, Tegenkamp C and Pfnür H 2003 The growth of NaCl on flat and stepped silver surfaces *J. Phys.: Condens. Matter* **15** 6473
- [23] Matthaei F, Heidorn S, Boom K, Bertram C, Safiei A, Henzl J and Morgenstern K 2012 Coulomb attraction during the carpet growth mode of NaCl *J. Phys.: Condens. Matter* **24** 354006
- [24] Repp J, Steurer W, Scivetti I, Persson M, Gross L and Meyer G 2016 Charge-state-dependent diffusion of individual gold adatoms on ionic thin NaCl films *Phys. Rev. Lett.* **117** 146102

- [25] Patera L L, Queck F, Scheuerer P and Repp J 2019 Mapping orbital changes upon electron transfer with tunnelling microscopy on insulators *Nature* **566** 245–8
- [26] Fatayer S *et al* 2019 Molecular structure elucidation with charge-state control *Science* **365** 142–5
- [27] Hernangómez-Pérez D, Schlör J, Egger D A, Patera L L, Repp J and Evers F 2020 Reorganization energy and polaronic effects of pentacene on NaCl films *Phys. Rev. B* **102** 115419
- [28] Katano S and Uehara Y 2020 *In situ* observation of atomic-scale growth of a NaCl thin crystal on Au(111) by scanning tunneling microscopy *J. Phys. Chem. C* **124** 20184–92
- [29] Reinert F, Nicolay G, Schmidt S, Ehm D and Hufner S 2001 Direct measurements of the L-gap surface states on the (111) face of noble metals by photoelectron spectroscopy *Phys. Rev. B* **63** 115415
- [30] Heidorn S, Bertram C, Koch J, Boom K, Matthaei F, Safiei A, Henzl J and Morgenstern K 2013 Influence of substrate surface-induced defects on the interface state between NaCl(100) and Ag(111) *J. Phys. Chem. C* **117** 16095–103
- [31] Dyer M S and Persson M 2010 The nature of the observed free-electron-like state in a PTCDA monolayer on Ag(111) *New J. Phys.* **12** 063014
- [32] Amsalem P *et al* 2013 Role of charge transfer, dipole–dipole interactions, and electrostatics in Fermi-level pinning at a molecular heterojunction on a metal surface *Phys. Rev. B* **87** 035440
- [33] Bagus P S, Staemmler V and Wöll C 2002 Exchangelike effects for closed-shell adsorbates: interface dipole and work function *Phys. Rev. Lett.* **89** 096104
- [34] Witte G, Lukas S, Bagus P S and Wöll C 2005 Vacuum level alignment at organic/metal junctions: ‘Cushion’ effect and the interface dipole *Appl. Phys. Lett.* **87** 263502
- [35] Cabailh G, Henry C R and Barth C 2012 Thin NaCl films on silver (001): island growth and work function *New J. Phys.* **14** 103037
- [36] Schultz T, Amsalem P, Kotadiya N B, Lenz T, Blom P W M and Koch N 2018 Importance of substrate work function homogeneity for reliable ionization energy determination by photoelectron spectroscopy *Phys. Status Solidi b* **256** 1800299
- [37] Schultz T *et al* 2017 Reliable work function determination of multicomponent surfaces and interfaces: the role of electrostatic potentials in ultraviolet photoelectron spectroscopy *Adv. Mater. Interfaces* **4** 1700324
- [38] Arkhestov R K, Alchagirov B B and Kegadueva Z A 2014 Electron work function of sodium: the current state of researches 2014 10th Int. Vacuum Electron Sources Conf. (IVESC) pp 1–2
- [39] Smith N V and Spicer W E 1969 Photoemission studies of the alkali metals: I. Sodium and potassium *Phys. Rev.* **188** 593–605
- [40] Wong K, Tikhonov G and Kresin V V 2002 Temperature-dependent work functions of free alkali-metal nanoparticles *Phys. Rev. B* **66** 125401
- [41] Szymonski M, Kolodziej J, Czuba P, Piatkowski P, Poradzisz A, Tolk N H and Fine J 1991 New mechanism for electron-stimulated desorption of nonthermal halogen atoms from alkali-halide surfaces *Phys. Rev. Lett.* **67** 1906–9
- [42] Such B, Czuba P, Piatkowski P and Szymonski M 2000 AFM studies of electron-stimulated desorption process of KBr(001) surface *Surf. Sci.* **451** 203–7
- [43] Seifert N, Ye H, Tolk N, Husinsky W and Betz G 1994 The influence of defects and defect clusters on alkali atom desorption stimulated by low energy electron bombardment of alkali halides *Nucl. Instrum. Methods Phys. Res. B* **84** 77–88
- [44] Szymonski M, Kolodziej J, Czuba P, Korecki P, Piatkowski P, Postawa Z, Piacentini M and Zema N 1996 Photon stimulated desorption from alkali halide surfaces at near threshold energies *Surf. Sci.* **363** 229–33
- [45] Höche H, Toennies J P and Vollmer R 1994 Combined electron-microscope surface-decoration and helium-atom-scattering study of the layer-by-layer photon-stimulated desorption from NaCl cleavage faces *Phys. Rev. B* **50** 679–91